Robotic System for Mapping 3D in-wall Information for Craftsmen

J. Vorndamme[1)], S. Petereit[2)], B. Pitzer[3)], P. Roan[3)], T. Lilge[1)], A. Albert[1)2)]

[1)] Institut für Regelungstechnik, Leibniz Universität Hannover, Germany
[2)] Robert Bosch GmbH, Corporate Research, Schwieberdingen, Germany
[3)] Robert Bosch LLC, Corporate Research, Palo Alto, USA

Abstract

This paper presents a robotic system for autonomously scanning wall surfaces by means of inductive, capacitive and AC measurements in order to gather information about flush-mounted power lines, water pipes and cavities. From these data the system generates a 3D map with in-wall information. Algorithms for surface scanning are described enabling robust methods for data acquisition and fusion of the scanning and localization data. The paper describes and evaluates two methods for reconstructing surface and in-wall information: The first one uses occupancy grid mapping along with the elaborated sensing model of the wall scanner, the second is a combination of scanning and mapping. The created 3D map is made available to a second system that projects the map onto the wall surface, removing distortions induced by the lack of a perpendicular projection. That system provides craftsmen the additional information to prevent hitting wires or water pipes when performing drilling tasks. The utilized robots make use of the robot software framework ROS.

Keywords: Autonomous wall scanning, in-wall information, flush-mounted piping and electric installations, sensor fusion and localization to a 3D-map, projection of in-wall information, SLAM, occupancy grid mapping, ROS

1 Introduction

Problems that arise in drilling tasks are often caused by hitting flush-mounted water pipes, power lines or cavities (e.g. in lightweight walls), which may lead to severe damages and costs. Although this in-wall information is of high importance for craftsmen, it is likely to be poorly documented, particularly for existing buildings. In order to assist craftsmen when drilling, we are developing an experimental robotic system consisting of two robot platforms. The first one autonomously generates a 3D map of the in-wall information (power lines, pipes etc.). For that purpose a wall scanner has been mounted on the robot and linear drives position the device appropriately on the wall in order to gather the required data. The second platform subsequently projects this in-wall information on the wall surface in order to assist the craftsmen. For that purpose a beamer is pivotally mounted on the robot.

Augmentation of information is already in use in other domains like military, medical science, or production. For example, relevant information is displayed during the repair of military vehicles in a head-up display [5], preoperatively acquired data is projected in minimal invasive intervention to help surgeons [7], or in manual welding processes the welding gun's position is suggested and errors are displayed [1]. The presented research aims to help establishing the augmentation in the domain of craftsmen by projecting in-wall information that is autonomously gathered in advance. Such an application is not known to exist yet. The paper is organized as follows: Section 2 gives a short description of the mobile projection system with the capability of undistorted projection of the map onto the wall surface. The scanning system is presented in detail in section 3. In addition, section 3 will discuss the sensor model of our wall scanner. Further a procedure for autonomously gathering in-wall information is presented. Section 4 then sketches how the fusion of robot sensor data is done with the wall scanner data in order to derive a 3D map. Two different approaches for generating the desired map of in-wall information are considered. Experimental results are presented in section 5. The paper ends with a summary and concluding remarks in section 6. Additionally, the next steps of the study are shortly sketched.

2 The projection system

The projection demonstrator is shown in **Figure 1** which is capable of automatically correcting distortions arising from non-orthogonal projections [3]. The mobile projection system uses 4 steerable drive wheels to provide an omni-directional platform. The platform is equipped with 2 laser scanners for localization of the robot, a pivotally mounted beamer for projection (3 degrees of freedom), and a stereo camera system, which together with the beamer is used to measure the robot heading towards walls.

Figure 2 shows the basic concept of the augmentation system. The main block of the augmentation is *computer vi-*

sion & image creation. It considers the 3D-map to be given and generates the image to be projected. For that purpose the original image is 'pre-warped', making use of the robot pose and the orientation of the robot towards the wall.

Figure 1: Left: Demonstrator for projection of in-wall information (mobile platform with traversable projector). Right: No distortion despite oblique projection

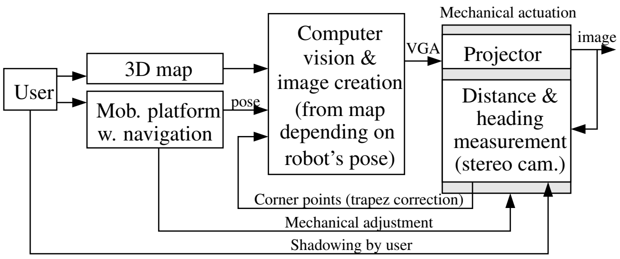

Figure 2: Basic concept for augmentation

The estimation of the robot's orientation towards the wall is illustrated in **Figure 3**. A square pattern is projected on the wall and computer vision algorithms are used to detect corners within this pattern. Stereo triangulation then delivers the respective coordinates in the camera frame.

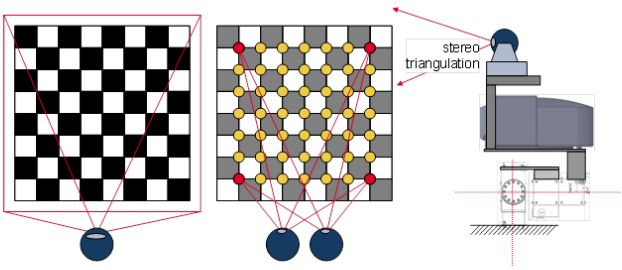

Figure 3: Estimation of the robot's orientation

Experiments with this system have shown, that under normal conditions (projector distance to wall $< 4\,\mathrm{m}$) a sufficient accuracy can be achieved. However, acceptable results on the accuracy of the detected corners in the projected square pattern require expensive and optically well adjusted cameras [3].

3 The scanning system

The scanning system is based on the same omni-directional platform as the projection system described in section 2. **Figure 4** shows a CAD sketch and a picture of the scanning system, equipped with 2 computer systems: One is used for controlling the platform itself and a second for gathering the data from the wall scanning device, fusing the scanning and localization data, and creating the map.
Two laser scanners are mounted at the base of the robot for localization and for navigating along walls. They are also used for preventing collisions (safety). Two linear drives mounted on the robot allow the scanning device to be positioned on the wall (xy-position). A passive spring-based mounting assembly ensures the scanner is positioned at a proper contact to the wall. An off-the-shelf wall scanner (GMS120, Bosch) is used. The device provides three sensors: Inductive, capacitive and alternating current sensing. In order to derive a measurement model the scanner was mounted on a position controlled sledge and moved along a prepared wooden plate. Behind the plate two copper pipes and a plugged-in extension cord were mounted at approximately 0.80 m, 1.40 m, and 0.35 m, respectively.

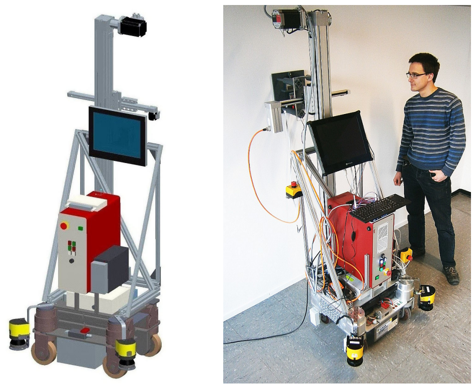

Figure 4: Mobile scanning system

The primary function of the capacity sensor is to detect wood beams whereas our task is to detect power lines and metal. Therefore, the capacitive sensor is not used during autonomous wall scans.
The following two diagrams show the sensor signal data of the inductive and AC sensors plotted over the sensor position. The sensor data (symbol α) is scaled for the display (hmi) of the scanning device by which the absolute values loose their physical meaning. The left edge of the plate is at position 0 m. In every plot three different measurements are plotted to give an impression of the variability of the sensors.
Figure 5 shows three different runs of the inductive sensor along the test wall. These measurements are highly reproducible. The second and third peaks are caused by the two pipes, while the first peak is caused by a mounting plate. The first pipe at approx. 0.8 m is mounted with an angle of $45°$ resulting in a slightly lower and wider peak in the sensor signal compared to the peak resulting from a vertically mounted pipe at approx. 1.4 m. The scan experiments have shown that every metallic material close to the scanner can falsify the measurements. It is therefore important not to

use metal for the holding of the scanning device in order to ensure correct behaviour of the inductive sensor. Further experiments have shown that metal within 15 cm of the device should be avoided.

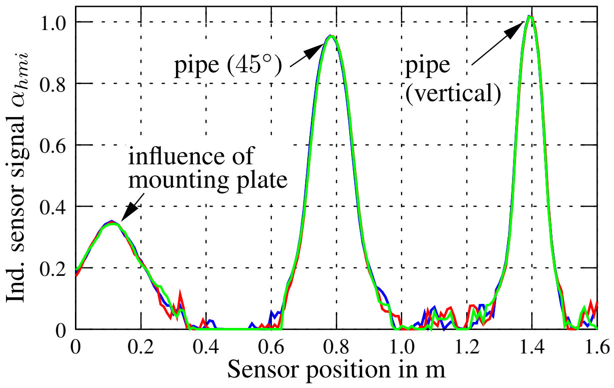

Figure 5: Inductive sensor data; different colors indicate different runs

Figure 6 finally depicts the values of the alternating current sensor. The reproducibility of these scans is even better compared to the inductive sensor. The power line at approx. 0.35 m produces a sharp peak which is exactly at the same position for all measurements. However, metal close to the power line seems to produce a constant sensor value at medium level, due to inductive coupling. This coupling can also be seen at the positions of the pipes (approx. at 0.8 m and 1.4 m) where the AC sensor gives a low signal due to the coupling from the power line. A slight deviation from inductive to AC measurement is due to some hysteresis of the inductive sensor, depending whether the pipe is approached from the left or the right.

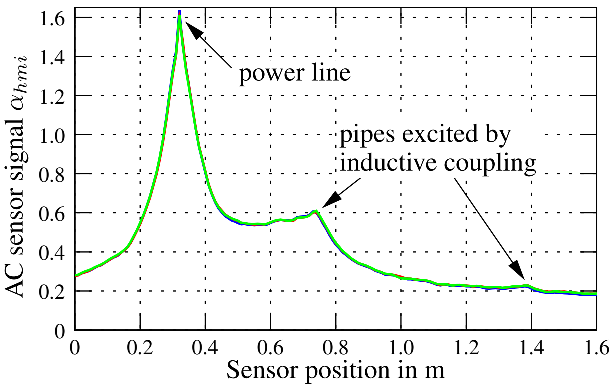

Figure 6: Alternating current sensor data (detection of a power line). Plots show high reproducibility.

Both sensors show appropriate results suitable for a pipe or power line detection with sufficient evidence. However, the inductive sensor is easily disturbed by metal near the scanning device. This has to be taken into consideration for the construction used for positioning the device. Additionally, the mutual sensitivity (inductive coupling of pipes visible in the AC measurements and copper wire of power lines visible in the inductive measurement) can be used to improve the sensor models. This fact can also be exploited by the later sensor data fusion and hence increase evidence and plausibility. So far we have, however, not considered these facts.

4 Mapping and Visualization

Basically two approaches were investigated throughout our experiments. The first approach makes use of an existing 3D model and applies occupancy grid mapping to associate the wall scanner data with the 3D model.
The second approach is to scan the wall by means of (rectangular) frames with a width of approx. 0.35 m and to stitch together these frames to the overall 3D map by means of an optimization problem.

4.1 Occupancy grid map approach

The goal of the system is to create a 3D in-wall information map that can be used by a craftsman. In order to create a consistent representation of the environment, sensor data from the wall scanner needs to be fused with 3D data, for example delivered from a stereo camera system or another 3D sensor. In this approach the Kinect is used.
The result is a surface representation of the wall that includes information about in-wall features. Surface representations are well suited for fast rendering, efficient data reduction, and semantic labeling. For these reasons, we use triangle meshes as our geometric and visual representation for 3D in-wall maps. In our system we triangulate the raw point cloud by exploiting the regular structure of the measurements. The scanning process already lays out the 3D input points in a grid like structure referred to as range image. A 3D mesh is created by connecting a point in the range image with two of its neighbors in each angular direction which yields a triangulation in the 2D range image space. Since we know the corresponding 3D position in space for each range image point, the 2D triangulation can be easily transferred into a 3D mesh. **Figure 7** depicts an example of a room corner captured by the scanning system and reconstructed as a surface mesh.

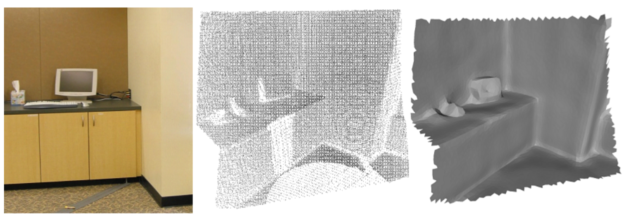

Figure 7: Left: Room corner. Middle: 3D Point Cloud. Right: Reconstructed Surface Mesh

The next step is to create a map of in-wall features that can be fused with the surface mesh. The input data for creating the map are the sensor signals from the wall scanner. An exemplary plot of a horizontal wall surface showing power line in-wall features is shown in **Figure 8**.

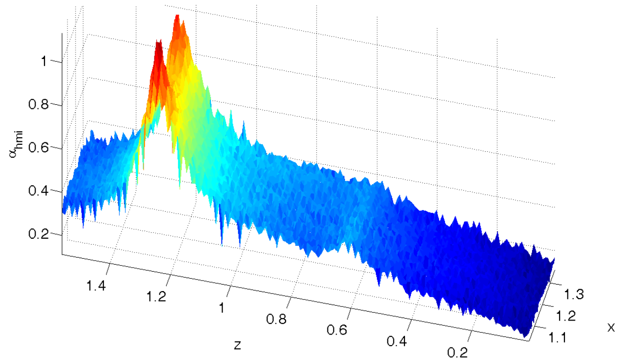

Figure 8: 2D scan of a wall fragment using the AC sensor. A horizontal power line is detected at $y \approx 1.25$ m as shown by the peaks in the scan

In this system we use a 2D surface map which can be applied to the 3D mesh as a texture. The basic idea for the in-wall mapping algorithm is to maintain an evenly spaced 2D grid structure g, where each cell g_i represents a random variable. Each random variable is binary and signals if an in-wall object is detected or not. This *occupancy grid mapping* approach [8] calculates the posterior over maps $p(g|\alpha, x)$, where α is the set of all measurements taken by the wall scanner and x are positions of the sensor on the wall. Due to the log odds representation new sensor data can be merged into the grid map by adding up the values in each individual grid cell. The occupancy grid map update requires defining an inverse sensor model that calculates the amount of evidence caused by a single measurement.

In our case, a simple inverse sensor model can be defined. We use a sensor model that increases the evidence for grid cells inside a measurement cone in case the measured value exceeds a defined threshold. This way grid cells accumulate more and more evidence with each measurement. In case the measured value is below the threshold the evidence for the cell not containing an in-wall object is accentuated.

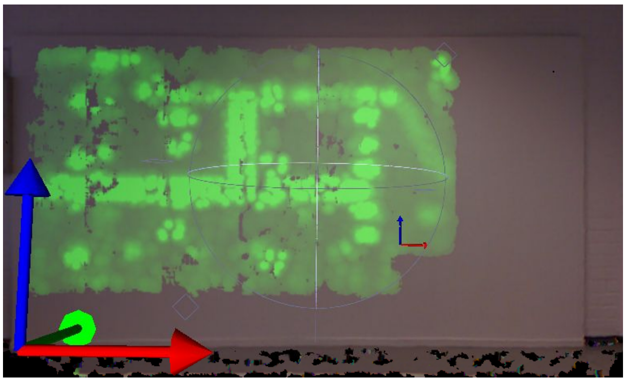

Figure 9: Exemplary result of occupancy grid map approach. Please refer to figure 14 for the true in-wall setup.

Figure 9 shows the result of this approach whereby the 3D map was captured by a Kinect device mounted on the robot together with the related ROS package [4]. The position of the wall scanner was calculated from the pose estimation of the mobile platform and the forward kinematics describing the wall scanner positioning device.

4.2 Combined scanning and 3D mapping

The method described in section 4.1 relies on an accurate map and particularly good localization of the wall scanner. In the following we will present another approach which breaks down the 3D mapping into some subtasks.
Figure 10 illustrates how the robot is positioned and scanning is accomplished. Basically, the laser scanners of the platform are used for the following tasks, namely the

- global localization (in the 2D map of the room),
- for relative localization with respect to the side walls giving information on the x-position with respect to the scanned wall, and
- for aligning the robot towards this wall.

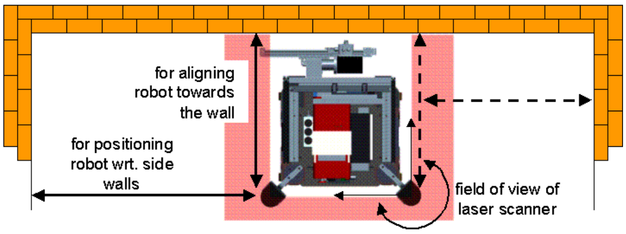

Figure 10: Top view on robot: Positioning and alignment of robot is based on laser scanners

Figure 11 shows the flow chart of the mapping process, i.e. association of the measurements within the map. Subsequently, the steps therein are described.

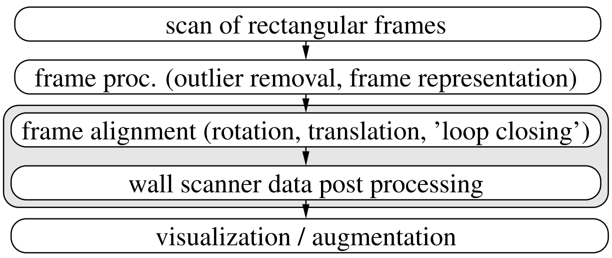

Figure 11: Flow chart of mapping procedure

Collecting rectangular scan frames

The position at which the scan data is acquired is derived from the robot localization solution and the forward kinematics of the wall scanner positioning device. Since the mobile system is in rest during a frame scan, there is a high consistency within the frame. However, uncertainties from one frame to the next are not negligible as can be seen in

Figure 12 (uncertainties in x, y, ϕ). In addition, the points close to the ground are distorted as some wires of the xy-positioning system are shadowing the laser scanners.

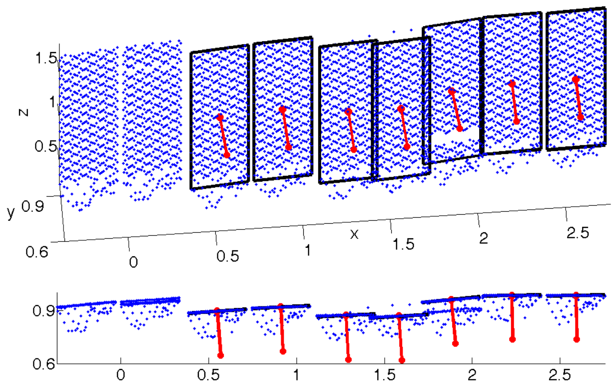

Figure 12: Point cloud of frames in 3D and top view with extracted planes of some frames

Therefore, first the plane can be extracted and outlier can be removed from the data by means of RANSAC [2] or similar fitting algorithms. Thereafter, the centre of gravity and orientation of the frame is calculated whereas the associated covariances is derived from the average values of the localization / navigation stack after removal of the outliers. **Figure 13** shows the top view of the representation of all scanned frames in a room.

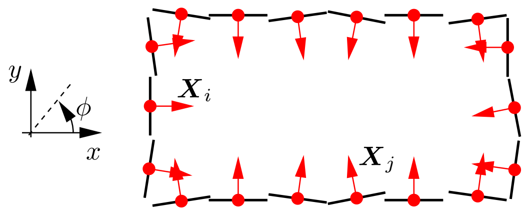

Figure 13: Frame representation by its pose $\boldsymbol{X}_i$

Frame alignment

Now the frames are aligned (stitched together). Basically, well known technologies from the 'loop-closing problem' are utilized (please refer for instance to [6]).
The frame positions are represented by a pose sequence $\boldsymbol{X}_i$. So called *constraints* introduce relationships between poses. One should bear in mind that *constraints* do not need to be fulfilled exactly, but in the probabilistic sense, i.e. due to the uncertainties the constraints are fulfilled with some probability but with no guarantee. The respective uncertainties are considered as to be normally distributed (Gaussian). Typically *constraints* are derived from following observations:

- odometry / localization between poses,
- sensing of identical features from two poses, or
- prior knowledge

Comparing *constraints* with observations leads to so called *residuals*. For the i-th residuum $\boldsymbol{r}_i$ one may write

$$\boldsymbol{r}_i = \boldsymbol{z}_i - \boldsymbol{f}_i(\boldsymbol{x})$$

whereas $\boldsymbol{z}_i$ represents the observation and $\boldsymbol{f}_i$ the *constraint*. Each *constraint* is associated with its own uncertainty $\boldsymbol{\Sigma}_i$ resp. its confidence $\boldsymbol{\Sigma}_i^{-1}$.
A set of poses that is best explained by all constraints can be calculated by minimizing the following sum of square errors (Mahalanobis-distances)

$$\xi^2 = \sum_i \xi_i^2 = \sum_i \boldsymbol{r}_i^T \boldsymbol{\Sigma}_i^{-1} \boldsymbol{r}_i$$

As *constraints* we use the localization solution delivered by the navigation stack and the relative position measurements of the laser scanner when the robot aligns to the wall. In our fairly 'collaborative' setup with rather bounded errors we can treat the problem linearly and solve it efficiently in matrix form. For that purpose we stack the vector of unknowns $\boldsymbol{x}$ and the confidence matrix $\boldsymbol{\Sigma}_S^{-1}$ and may reformulate our residual vector $\boldsymbol{r} = \boldsymbol{z} - \boldsymbol{J}\boldsymbol{x}$ with the stacked Jacobian $\boldsymbol{J}$. Our loss function becomes

$$\xi^2 = \sum_i \xi_i^2 = (\boldsymbol{z} - \boldsymbol{J}\boldsymbol{x})^T \boldsymbol{\Sigma}_S^{-1} (\boldsymbol{z} - \boldsymbol{J}\boldsymbol{x})$$

and minimization leads to the solution

$$\boldsymbol{x} = (\boldsymbol{J}^T \boldsymbol{\Sigma}_S^{-1} \boldsymbol{J})^{-1} \boldsymbol{J}^T \boldsymbol{\Sigma}_S^{-1} \boldsymbol{z}$$

Wallscanner data post processing

Finally, the wall scanner data can be post processed by computer vision methods in order to smooth transitions and to sharpen the results if necessary. In our experiments so far there was no need for further processing.

5 Experimental results

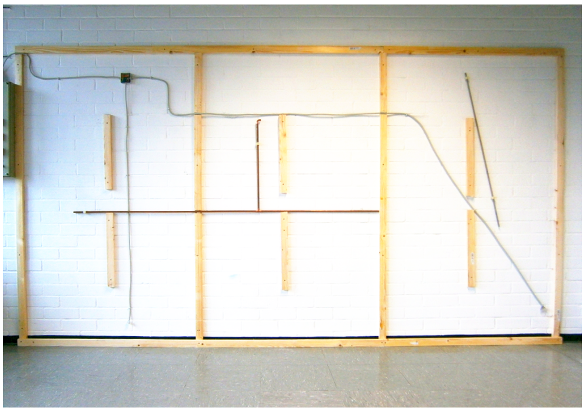

Figure 14: Picture of the in-wall information prior to plaster work

Figure 14 shows as a reference the picture of the experimental wall prior to plaster work. As can be seen it consists of some horizontal, vertical and diagonal power cables as well as of copper pipes with changing orientations. **Figure 15** illustrates the result after accomplishing all mentioned steps in section 4.2. The high performance of the used device is indicated by the small peaks which are due to screws and nails from the wooden structure and the cable clamps, respectively.

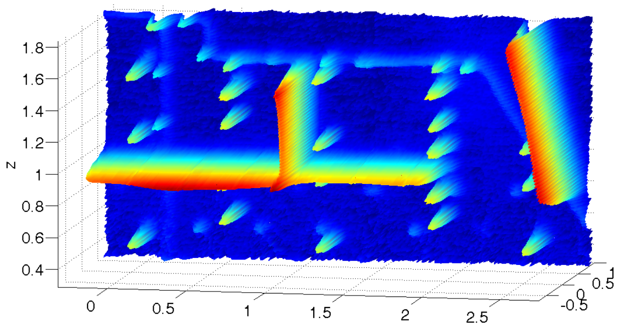

Figure 15: Results after frame alignment (ind. sensor)

Finally, **Figure 16** overlays the real picture with the result of the in-wall 3D map. The scan of the shown area takes approx. 5.5 hours to complete with our yet not optimized scanning process.

Figure 16: Picture of the wall with overlaid inductive scan results (highlighted by a frame)

6 Summary and conclusions

This work has shown a new application for a robotic system, namely the autonomous scanning of wall surfaces in order to generate a 3D map with in-wall information like flush-mounted power lines and water pipes. Two methods to generate such a map have been investigated: The one uses occupancy grid mapping, and the other a combination of scanning and mapping. Results are promising from both approaches; hence, both we will further investigate and optimize. The main differences are as follows:

Grid Mapping

+ online visualization directly within wall picture
+ allows different inverse sensor models
+ robust against measurement noise
– accuracy highly depends on grid quality (robot's localization and camera position)

Scanning and Mapping (with loop closing)

+ more accurate, depending on localization
+ no tuning of parameters
+ visualization and data storage in map coordinates
– requires preprocessing of data $\rightarrow$ higher effort
– no online visualization

The scanning device proved very accurate - even screws and nails can be detected and localized accurately. Such objects may in the future be used as additional features to increase map accuracy.

Due to cross-sensitivity of the measurement principle - e.g. the inductive sensor can as well detect power lines (which contain copper) - several maps with alignable information exist. In the future we will fuse these data appropriately. Additionally, model based approaches for the scanning itself will be developed in order to ensure time efficiency of the process.

References

[1] D. Aiteanu, B. Hillers, and A. Gräser. A step forward in manual welding: demonstration of augmented reality helmet. In *Mixed and Augmented Reality, 2003. Proceedings. The Second IEEE and ACM International Symposium on*, pages 309 – 310, oct. 2003.

[2] M. A. Fischler and R. C. Bolles. Random Sample Consensus: A paradigm for model fitting with applications to image analysis and automated cartography. *Communication of the ACM*, 24(6):381 – 395, 1981.

[3] D. Gaudig. Autonome Projektionseinrichtung zur Augmentierung der Arbeitsumgebung im Innenausbau, (in German). Master's thesis, Robert Bosch GmbH with University Stuttgart, 2009.

[4] S. Gedikli, P. Mihelich, and R. B. Rusu. A ros driver for openni depth (+ rgb) cameras, 2011. http://ros.org/wiki/openni_camera, 2012-03-14.

[5] S. Henderson and S. Feiner. Evaluating the benefits of augmented reality for task localization in maintenance of an armored personnel carrier turret. In *Mixed and Augmented Reality, 2009. ISMAR 2009. 8th IEEE International Symposium on*, pages 135 –144, oct. 2009.

[6] K. Konolige. Large-scale map-making. In *Proceedings of the National Conference on AI (AAAI)*, 2004.

[7] B. Schwald, H. Seibert, M. Schnaider, S. Wesarg, and R. Röddiger. Implementation and evaluation of an augmented reality system supporting minimal invasive interventions. In *Workshop AMI-ARCS*, pages 41–48, Rennes, France, 2004.

[8] S. Thrun. Learning occupancy grid maps with forward sensor models. *Autonomous Robots*, 15(2):111–127, 2003.